PERGAMON

International Journal of Solids and Structures 37 (2000) 1403–1423

INTERNATIONAL JOURNAL OF SOLIDS and STRUCTURES

www.elsevier.com/locate/ijsolstr

Ballistic limit of metal plates struck by blunt deformable missiles: experiments

Dongquan Liu, W.J. Stronge*

Department of Engineering, University of Cambridge, Trumpington Street, Cambridge CB2 1PZ, UK

Received 3 December 1997; in revised form 4 November 1998

Abstract

A soft or deformable missile changes shape as it penetrates a ductile metal target. The deformation increases the area of the contact surface and thus decreases the areal density of the missile. This paper investigates the effect of relative deformability of missile and plate on the ballistic limit of thin ductile plates which are struck at normal obliquity by soft cylindrical missiles. The effect of various parameters on the extent of global deformation (dishing) and localised failure mechanisms of the target plate are examined as a function of the relative size of plate and missile, flow stress and fracture strain of the plate, missile mass, missile deformability at impact speeds close to the ballistic limit. There also is an analysis of how these deformation and failure characteristics affect the ballistic limit of a target plate.

1. Introduction

Accidental impact scenarios frequently involve missiles that are composed of relatively soft materials. Bird strike and the impact of hail stones on aircraft are examples of impact by soft missiles. Another example is accidental explosions where the risk of puncturing nearby pipes or panels by hurled fragment can depend on the relative hardness of the fragments in comparison with that of the pipe or panel that they strike. The present research is to assess resistance of ductile metal plates to perforation by cylindrical missiles of different hardnesses striking at normal incidence with impact speeds V_0 in the subordnance velocity range ($25 < V_0 < 500$ m/s (Backman and Goldsmith, 1978)). The resistance of a plate to perforation can be represented by an important parameter, the *ballistic limit*; i.e. the minimum impact speed where the missile perforates the plate. In the 'subordnance' velocity range, impact of missiles can cause both global deformation and localised failure of the target plate. The global deflection surrounding the impact point is defined as 'dishing'. For thin to moderately thick ductile metal plates

* Corresponding author. Fax: +44-1223-332-662.
E-mail address: wjs@eng.cam.ac.uk (W.J. Stronge).

0020-7683/00/$ - see front matter
PII: S0020-7683(98)00322-9

struck by blunt missiles, dishing first occurs and then the subsequent failure mechanism is either 'plugging' (predominantly shear rupture) or 'discing' (predominantly tensile rupture)[1]. Ruptures develop in a narrow annulus around the contact area; the dominant rupture depends on the extent of the structural deformation or dishing (Liu, 1996). A large stretching strain in the narrow annulus as a consequence of very large structure deformation (dishing) results in a failure of the plate by discing. In contrast, in the case of very little structural deformation, a plate fails by plugging due to a large relative transverse displacement between the plug underneath the missile and the surrounding plate. As shown by Liu and Stronge (1995), the ballistic limit of a metal plate struck by a blunt missile in the subordnance velocity range cannot be predicted correctly without relating the localised failure mode (either discing or plugging) to the extent of structural deformation.

A deformable missile can be either hard and relatively undeformable or ductile and very deformable in comparison with a target plate. As a ductile missile penetrates a metal plate the impact end of missile spreads radially or mushrooms. The mushrooming of a ductile missile striking a rigid target was analysed by Whiffin (1948) and Taylor (1948). In the ordnance velocity range ($500 < V_0 < 1300$ m/s), some experiments were conducted to investigate the penetration and perforation behaviour of metal plates by ductile missiles (Recht, 1978; Woodward and DeMorton, 1976). In these experiments, the target plates underwent little structural deformation away from the impact point; the investigation was focused on size of the hole produced by the mushroomed missile and how this affected the residual velocity of the missile after perforation. In the subordnance speed range, Corran et al., (1983) gave an simple example where a soft missile resulted in a larger ballistic limit than that of a hard missile for impact against an identical thin metal plate.

In the subordnance impact speed range, previous experiments focused on effects of plate material properties and the relative size of missile and plate. The effect of missile deformability was neglected by using a very hard missile so there was little plastic deformation generated in the missile during the impact process. Although there have been many papers which examined the deformation and failure behaviour of ductile metal plates struck by hard missiles, the following two problems remain.

1. It has not been made clear how the ratio of plate thickness to missile diameter and the plate fracture strain affect the failure mechanism of a target plate struck by a flat-ended missile. Corran et al. (1983) suggested that target plates of mild steel, stainless steel and aluminium alloy struck by flat-ended missiles failed by 'plugging' for ratios of plate thickness to missile radius H/r_m in the range $0.168 < H/r_m < 1.0$; they did not discuss the effect of the plate material ductility on rupture. In contrast, Lethaby and Skidmore (1977) concluded that for mild steel plates, the failure mechanism was discing if $0.168 < H/r_m < 0.34$.
2. The experimental data for the ballistic limit has been interpreted in relation to missile mass, plate yield stress, plate thickness and missile radius but not in relation to the ductility of the plate material (Corbett et al., 1996).

The present paper mainly reports data for the ballistic limit of ductile metal plates struck by blunt missiles at normal incidence with incident speeds in the subordnance velocity range. In these experiments the missiles are made from materials with different hardness ranging from a soft polymer (PTFE) to hardened steel. The influence of various non-dimensional parameters on the extent of global

[1] Stronge, (1985) described discing as 'a circumferential fracture near the periphery of the impressed region that results from radial stress associated with dishing of the (thin) plate'. This through-thickness mode of failure was further investigated by Palomby and Stronge (1988). Use of the term 'discing' by Woodward (1979) describes an alternative failure mode in moderately thick plates which have low fracture toughness across planes parallel to the surface—a failure mode that has the appearance of spalling.

Table 1
Plates and missiles in first group of tests

Plate			Missile	
Material	Thickness mm	Diameter mm	Mass g	Diameter mm
1200 aluminium	1.22, 3.03, 6.42	95	3.8	12.5
1200 aluminium	1.22, 3.03, 6.42	95	9.7	12.5
2014A TB	3.25, 6.27	95	23.6	12.5
Mild steel	1.15, 2.98, 6.10	95	23.6	12.5
Mild steel	1.15, 2.98	95	23.6	25.0
Mild steel	1.15, 2.98	190	23.6	12.5

deformation and type of localised failure mechanisms of target plates are examined as functions of the relative size of plate and missile, plate flow stress and fracture strain, missile mass, and deformability for ductile missiles. Later there is a discussion of how these deformation and failure characteristics affect the ballistic limit of the plates.

2. General details

2.1. Description of experiments

To examine the effects of various parameters on the ballistic limit, two groups of tests were conducted. The first group of tests consisted of firing hardened steel missiles against thin circular plates. These tests investigated perforation of plates made from three different materials: 1200 aluminium, 2014A TB aluminium alloy and mild steel. The hardened steel missiles experienced negligible inelastic deformation during the impact process and consequently can be considered as 'rigid' missiles. In these tests the missile mass, missile radius, plate material and plate thickness were varied within ranges listed in Table 1. These tests aimed to obtain general relations for the ballistic limit of target plates that are perforated by a hard flat-nosed cylindrical missile striking at a normal angle of obliquity. A second group of tests were conducted to examine the effects of deformability (mushrooming) of a ductile missile on the perforation behaviour and the ballistic limit of ductile aluminium plates. To achieve an extensive range of missile deformation characteristics, the tests in the second group were performed with soft or ductile missiles made of materials such as PTFE, 1200 aluminium, 6063 TF and 6061 T6 aluminium alloys. Those missiles all had mass of 3.8 g and a diameter 12.5 mm, so attention was focused on the influence of missile deformability. The targets in the second group were 1200 aluminium plates of thicknesses 1.22 and 3.03 mm. In both groups of tests, missiles struck the centre of the target plates at normal obliquity. The target plates were bolted in a specially designed mount that clamped the edge and restrained radial displacement; this resulted in a circular plate of diameter 95 mm. The plate diameter was 7.6 times the diameter of the missile. When the plate diameter was changed from 95 to 190 mm, the change in the ballistic limit of the mild steel plates of thickness 1.22 and 3.03 mm was less than 5%. This indicates that the plate size was sufficiently large that the boundaries had negligible influence on strains in the rupture zone. A nitrogen gas gun with an inner diameter 28.7 mm was used to accelerate the missiles to speeds above 25 m/s. Sabots made of Delron were used to carry missiles of diameters 12.5 and 25 mm down the barrel. The sabot was stripped off the missile by a stopper located just downstream of the muzzle. Missile velocities were controlled by either the gas pressure in the high

Table 2
Summary of material parameters of plates and missiles where ρ is mass density per unit volume, H is plate thickness, σ_y is yield stress, σ_u is ultimate stress, P is plastic strain hardening modulus, λ is strain rate hardening coefficient, e_u is ultimate strain, e_f is fracture strain. Data for strain rate hardening coefficient are from Shadbolt et al. (1983) and Walley et al. (1989)

	Material	ρ	H	$\sigma_y(Y)$	σ_u	P	λ	e_u	e_f
		g/cm^3	mm	N/mm^2					
Target plate	Mild steel	7.8	1.15	175	288	—	40	0.28	1.36
	Mild steel	7.8	2.98	371	485	—	40	0.17	1.00
	Mild steel	7.8	6.10	365	481	—	40	0.24	0.98
	2014A TB	2.7	3.25	302	464	—	4	0.18	0.40
	2014A TB	2.7	6.27	288	309	—	4	0.06	0.38
	1200 al.	2.7	1.22	106	112	—	—	0.03	1.05
	1200 al.	2.7	3.03	115	127	—	—	0.06	1.07
	1200 al.	2.7	6.42	114	125	—	—	0.04	1.20
Cylindrical missile	1200 al.	2.7	—	60	—	150	—	—	—
	6063 TF	2.7	—	150	—	200	—	—	—
	6061 T6	2.7	—	320	—	650	—	—	—
	PTFE	2.17	—	8	—	40	2.5	—	—

pressure cylinder that powers the gun or by initially locating the missile partway down the barrel before firing. The muzzle velocity of the missiles was measured by a digital timer which measured the time elapsed between the breaking of two sets of graphite leads that spanned the barrel at the muzzle; the distance between the break-wires was 50 mm.

2.2. Properties of plate and missile materials

2.2.1. Plate material properties

To measure material properties, quasi-static uniaxial tensile tests of strips cut from the same sheets as target plates and compressive tests of cylinders from the same rods as the deformable missiles were carried out in an Instron test machine. For the plate materials, the yield stress σ_y at 0.2% strain, ultimate stress σ_u, ultimate strain at maximum stress e_u and fracture strain e_f that are measured in uniaxial tensile tests are listed in Table 2. The fracture strain was measured from the change in width and thickness of the fractured section. This characteristic strain at fracture is defined as $e_f = A_0/A_f - 1$ where A_0 was the initial cross-sectional area and A_f was the smallest cross-sectional area of the necked region. The area of a deformed cross-section A_f was calculated from the mean width and thickness where the mean width and thickness were obtained by averaging those measurements at the edge and centre of the associated surface. The edge and central widths and thicknesses were measured with electrical vernier calipers.

2.2.2. Missile material properties

Because the deformable missiles suffered a predominantly compressive deformation in the impact process, the parameters from uniaxial compressive tests were essential for missile materials. These missile materials have elastic–plastic stress–strain relations. The plastic behaviour of the missile can be approximated by a rigid-plastic engineering stress–strain relation as follows (Recht, 1978) (Fig. 2)

Table 3
Experimental data of 1200 aluminium, 2014A TB aluminium and steel plates struck by hardened steel flat-ended missiles where M is missile mass, D_m is missile radius, H is plate thickness, D is plate radius, V_0 is missile incident velocity and V_b is the ballistic limit. Final state of perforation is indicated by (Y) perforated, (C) through thickness cracking or (N) no perforation

M g	D_m mm	Plate material	H mm	D mm	V_0 m/s	Perf. Y/C/N	V_b m/s
23.6	12.5	steel	1.15	95	77	C	81 ± 4
					85	Y	
23.6	12.5	steel	2.98	95	182	N	186 ± 4
					190	Y	
23.6	12.5	steel	6.10	95	268	C	287 ± 19
					306	Y	
23.6	12.5	steel	1.15	190	82	C	84 ± 2
					86	Y	
23.6	12.5	steel	2.98	190	180	N	181 ± 1
					182	Y	
23.6	25.0	steel	1.15	95	132	C	134 ± 2
					136	Y	
23.6	25.0	steel	2.98	95	305	N	314 ± 9
					323	Y	
23.6	12.5	2014A	3.25	95	117	C	122 ± 5
					127	Y	
23.6	12.5	2014A	6.27	95	144	C	147 ± 3
					151	Y	
9.7	12.5	1200 al.	1.22	95	53	N	56 ± 3
					59	Y	
9.7	12.5	1200 al.	3.03	95	141	N	144.5 ± 3.5
					148	Y	
9.7	12.5	1200 al.	6.42	95	213	N	218 ± 5
					223	Y	
3.8	12.5	1200 al.	1.22	95	94	N	97 ± 3
					100	Y	
3.8	12.5	1200 al.	3.03	95	224	N	229.5 ± 5.5
					235	Y	
3.8	12.5	1200 al.	6.42	95	352	N	357.5 ± 5.5
					363	Y	

$$\sigma = \frac{Y}{1-e} - P\frac{\ln(1-e)}{1-e} \tag{1}$$

where e is the axial component of engineering strain for a cross section. Values of missile yield stress Y and plastic strain hardening modulus P are listed in Table 2.

Mild steel and PTFE are materials which are sensitive to strain rate. A strain rate hardening coefficient λ for these materials is needed to calculate the dynamic flow stress or yield stress. The flow stress is defined as the average of the yield stress at 0.2% plastic strain and ultimate stress in a tensile stress–strain relation. The relation between dynamic flow stress σ_0^d (for a plate) or yield stress (σ_y^d for a plate and Y^d for a missile) and strain rate is expressed by (Lindholm, 1964; Shadbolt et al., 1983; Swallow et al., 1986; Walley et al., 1989)

$$\sigma_0^d = \sigma_0 + \lambda \log_{10}\dot{e} \tag{2}$$

Table 4
Experimental data of 1200 aluminium plates of diameter 95 mm struck by PTFE, 1200 aluminium, 6063 TF and 6061 T6 aluminium alloy missiles of diameter 12.5 mm where X is the final height of undeformed part and L_f is the final height of the entire missile. D_n, D_c and D_f are denoted in Fig. 1

Missile material	M g	H mm	V_0 m/s	Perf. Y/C/N	D_n mm	D_c mm	D_f mm	X mm	$L_f - X$ mm	V_b m/s
PTFE	3.8	1.22	126	N	12.84	—	—	9.40	4.52	129 ± 3
			132	Y	13.05	—	—	4.89	8.90	
PTFE	3.8	3.03	400	N	12.52	16.12	20.01	2.41	8.48	401.5 ± 1.5
			403	Y	13.00	16.45	19.75	3.08	8.50	
1200 al	3.8	3.03	347	C	—	—	18.0	6.0	3.6	354 ± 7
			361	Y	—	—	17.6	5.7	3.9	
6063 TF	3.8	3.03	312	N	—	—	15.2	5.4	4.9	319 ± 7
			327	Y	—	—	15.5	5.7	4.6	
6061 T6	3.8	3.03	243	N	—	—	13.0	3.5	7.7	247 ± 3
			251	Y	—	—	3.4	7.8	13.1	

or

$$\sigma_y^d = \sigma_y + \lambda \log_{10}\dot{e} \quad \text{or} \quad Y^d = Y + \lambda \log_{10}\dot{e} \tag{3}$$

Values of the strain rate hardening coefficient λ for these materials are listed in Table 2.

2.3. Experimental results

Table 3 gives the perforation data for 1200 aluminium, 2014A TB aluminium alloy and steel plates struck by hardened steel missiles at either the highest velocity giving partial perforation or the lowest velocity giving a complete perforation; Table 4 gives the data for 1200 aluminium plates struck by soft missiles. Symbol D_n is the diameter of plug around which necking occurs, D_c is the diameter of the crater (the area of obvious indentation) and D_f is the diameter of the contact area (Fig. 1); D_f is equal to the maximum diameter of the impact end of a ductile missile which has mushroomed. For a particular missile, the ballistic limit is approximated by the average of the highest velocity giving partial perforation and the lowest velocity giving a complete perforation.

3. Discussion 1: structural deformation and rupture of metal plates

Failure mechanisms observed in our experiments are discing and plugging. For an impact system with varying material and geometrical parameters, there are a variety of failure mechanisms. Failure

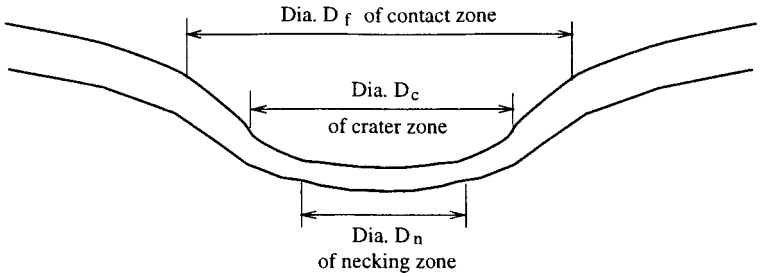

Fig. 1. Different regions in the impact zone.

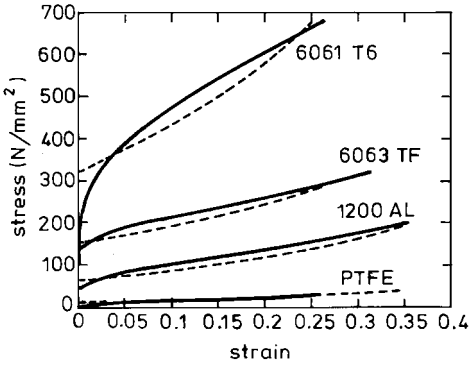

Fig. 2. Stress–strain relations of 1200 aluminium, 6063 TF and 6061 T6 aluminium alloys in uniaxial compressive tests. ——: experimental curves. - - -: best fit based on Eq. (1)

mechanisms are reported only for the plates struck by missiles at velocities close to the ballistic limit. To calculate the ballistic limit for any particular failure mechanism, a rupture criterion will be used to determine an upper bound on plate deformation near the periphery of the interface between plate and missile. In the following section, influences of several parameters on deformation and failure mechanisms of metal plates are examined separately.

3.1. Effects of plate thickness and missile radius

The effects of plate thickness and missile radius on the extent of global deformation and localised failure mechanisms of target plates were examined with several different thicknesses for each of the three plate materials (1200 aluminium, 2014A TB and mild steel). These plates were struck by hardened steel flat-ended missiles of diameters 12.5 and 25 mm; the corresponding ratios of plate thickness to missile radius ranged from 0.0435 to 1. With an increasing ratio of plate thickness to missile radius, a missile striking at a velocity close to the ballistic limit decreases the global deformation of the plate of the same material and is more likely to cause rupture due to shear strain (Fig. 3). For the ratios of plate thickness to missile radius less than 0.5, a representative fracture mechanism is shown in Fig. 4a. Fig. 4a illustrates that the fracture surface was at approximately 45° to the deformed surface of the plate. A similar fracture mechanism was observed by Lethaby and Skidmore (1974) for ratios of plate thickness

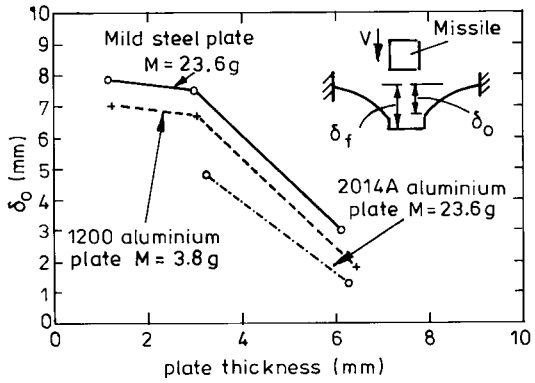

Fig. 3. Dishing of the plate just outside the plug δ_0 at impact speed V_0 slightly below the ballistic limit.

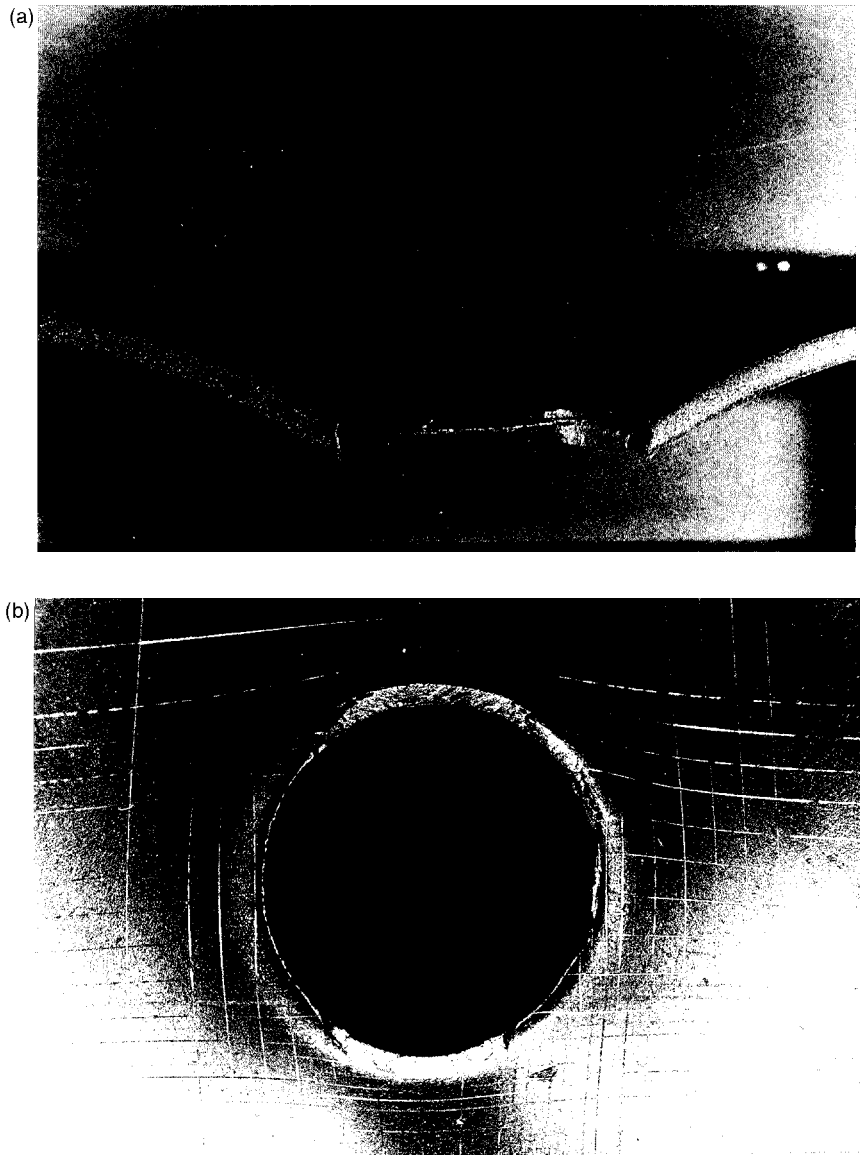

Fig. 4. Discing failure in a mild plate 2.98 mm thick struck by a hardened steel missile of radius 25 mm at 323 m/s; the fracture surface is at 45° to the plate surface. (a) Cross-sectional view; (b) top view.

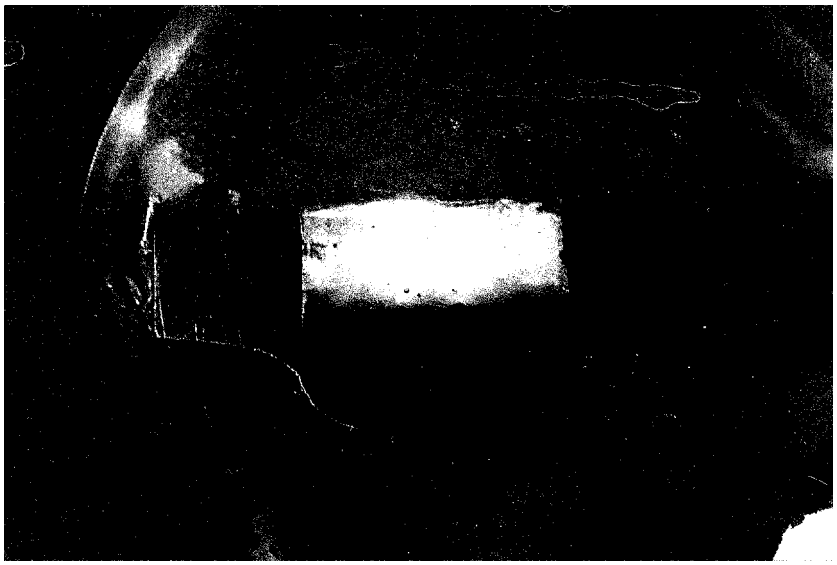

Fig. 5. A 1200 aluminium plate 6.42 mm thick struck by a hardened steel missile of diameter 12.5 mm and mass 3.8 g where ratio of the incident velocity to the ballistic limit is 0.98. Cross-section view shows a small shear crack in the upper part of the generalised hinge band.

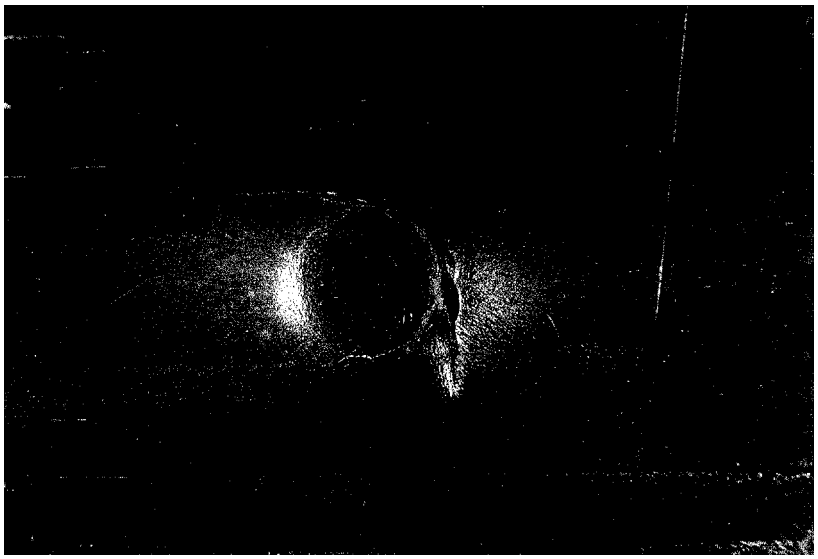

Fig. 6. Back view of rupture of a 2014A TB aluminium alloy plate of thickness 3.25 mm struck by a hardened steel missile of 23.6 g at a velocity 117 m/s.

to missile radius less than 0.34; the missiles were flat ended. They suggested that maximum shear strain occurred at approximately 45° to the plate surface and final rupture occurred when the radial stretching strain reached a critical value. Correspondingly, Fig. 4b shows that a large tensile strain occurred on the distal surface. As discussed by Liu and Stronge (1995), this failure mode is classified as discing because it is fundamentally caused by a large tensile strain due to stretching as well as bending. Dienes and Miles (1977) also concluded that membranes or thin plates struck by flat-ended missiles were ruptured by discing.

For the plate materials in these experiments, if the plate thickness is as large as the missile radius, the rupture mechanism is 'plugging' where the fracture surface is transverse to the plate surface (Fig. 5). With increasing plate thickness, the failure model changes from 'discing' to 'plugging' for a plate struck by flatended missiles. Analysis performed by Liu (1996) shows that the transition from discing to plugging occurs at a ratio of plate thickness to missile radius that is roughly equal to 0.59 for 2014A TB aluminium alloy plates or 0.5 for 1200 aluminium and mild steel plates. The effect of plate ductility on the failure mechanism of a target plate is discussed in the following subsection.

3.2. Effect of fracture strain of plate material

Based on experimental results for aluminium alloy and mild steel plates struck by flat-ended missiles ($0.22 < H/r_m < 1.37$ and $R/r_m = 14.14$) (Jones, 1995; Langseth and Larsen, 1990, 1994), Jones concluded that aluminium alloy plates are more likely to rupture by discing than are mild steel plates of the same thickness. The present experiments also suggested that 2014A TB aluminium alloy plates are more likely to fail by discing than 1200 aluminium and mild steel plates (Fig. 6) for the same ratio of plate thickness to missile radius. Aluminium alloy has small fracture strains (about 0.5) while 1200 aluminium and mild steel have large fracture strains (>1); this suggests that at the same ratio of impact speed to the ballistic limit V_0/V_b, a plate of smaller fracture strain is more likely to rupture by discing.

Another phenomenon observed from the present experiments is that for thin 2014 aluminium alloy plates that have a small value for the fracture strain, there is a multi-path cracking failure mechanism (a crack propagated away from the periphery along a tangent to the contact area) (Fig. 6). This phenomenon for aluminium alloy plates has been reported for ratios of plate thickness to missile radius less than 0.2 (Langseth and Larsen, 1994). However this phenomenon has not been observed for mild steel and 1200 aluminium plates and the difference may be that these materials have a large fracture strain.

3.3. Effect of missile mushrooming

To explain how the radial expansion of soft or ductile missiles affects the plate deformation and failure mechanism, a missile deformability index is proposed to represent the relative strength of the plate in comparison with the missile at impact velocities close to the ballistic limit. This index is $\rho_m V_{b1}^2/Y$ where ρ_m is missile mass density per unit volume, Y is the missile dynamic yield stress and V_{b1} is the ballistic limit of an identical plate struck by a hardened steel missile of the same diameter and mass as the specimen missile. If a ductile cylinder strikes end-on against a rigid surface, the enlarged area of the impact end of the cylinder is a function of $\rho_m V^2/Y$ where V is the impact velocity of the cylinder against the rigid surface (Taylor, 1948). The missile deformability index[2] $\rho_m V_{b1}^2/Y$ is a measure of missile radial expansion at the ballistic limit V_{b1}. The term $\rho_m V_{b1}^2$ represents the target strength (i.e. resistance to missile perforation) and is a function of plate yield stress, fracture strain and so on.

[2] This parameter is different from the damage number $\rho V^2/\sigma_y$ proposed by Johnson where σ_y is the yield stress of the target plate and V is the missile impact speed.

The ballistic limit for a ductile missile V_{b2} is non-dimensionalised with respect to a minimum speed $V_p = 2H\sqrt{\pi\sigma_0 e_f r_m/M}$ at which a hard missile of radius r_m and mass M perforate a rigid target plate; the symbol σ_0 is the plate static flow stress and H is the plate thickness. The speed V_p is termed the plugging speed. A detailed discussion of the plugging speed V_p is presented in Section 4.1. In Fig. 11, it can be seen from our experiments that for a soft missile the ratio of the ballistic limit V_{b2} to the plugging speed V_p is a function of the missile deformability index[3]. An alternative parameter $\sigma_y H/Yr_m$ based on pure plugging could be used to express the relative strength of plate to missile. However, data on the non-dimensional ballistic limit for plates of different thicknesses show that the alternative parameter does not eliminate dependence on plate thickness as successfully as the missile deformability index $\rho_m V_{b1}^2/Y$. In the present tests, the missile deformability index ranges from 0 to 9. In calculating the missile deformability index for aluminium missiles, the effect of strain rate on the yield stress is negligible. However for a PTFE missile, a dynamic yield strength is obtained from eqn (3) because PTFE is very sensitive to strain rates. The average strain rate is calculated based on a formula in Appendix A. For the PTFE missile striking at 400 m/s, the same deformability index has been applied despite many cracks appearing at the impact end of the missile.

In our experiments if the missile deformability index was less than 0.45 there was negligible radial expansion of a ductile missile striking a plate at a speed close to the ballistic limit (Figs. 7b, 8b, 9a and 9b); consequently, the extent of deformation and the type of failure mechanisms of a target plate was hardly affected by missile deformability (Figs. 9a and 9b). In the range of the missile deformability index larger than 0.45, the contact area increased and bending deformation developed at the impact end of a missile after it struck at a speed just below the ballistic limit (Figs. 9a and 9b). The larger radial expansion and bending deformation at the impact end of a softer missile led to a larger global deformation of the target plate and a failure mode that was controlled by radial tensile strain rather than shearing (Figs. 7a and 8a).

4. Discussion 2: ballistic limit of metal plates

The above section discusses how geometrical and material parameters influence the deformation and failure behaviour of a target plate. In this section we examine the manner in which this deformation and failure behaviour affect the ballistic limit of a target plate.

4.1. Effect of size and material parameters

For a plate struck by a hard missile of mass M at a speed equal to the ballistic limit V_b, the missile incident kinetic energy $MV_{b1}^2/2$ is a measure of global deformation of the plate. This kinetic energy is absorbed by (a) structural deformation (dishing) of the plate in the region surrounding the area of contact between the missile and plate, and (b) localised deformation of the narrow hinge band surrounding the plug. If the width of the hinge band around the plug is assumed to be equal to the plate thickness H (Liu and Stronge, 1995; Wen et al., 1995; Shen and Jones, 1992), perforation occurs when the local plastic work in the generalised hinge band is $2\pi\sigma_0 e_f r_m H^2$ regardless of whether the local

[3] Ratios of plate thickness to initial missile radius H/r_m for the two plate thicknesses tested are 0.49 and 0.19. As shown in Fig. 10 for hard missile impact cases (along the axis of zero missile deformability index in Fig. 11), ratios of the ballistic limit to plugging speed are very close for $H/r_m = 0.19$ and 0.49. However, for a thick plate (e.g., $H/r_m = 1$) struck by a hard missile the ratio of the ballistic limit to plugging speed is different from that for a thin plate (e.g., $H/r_m = 0.19$). To make the curve for a thick plate close to that for a thin plate in Fig. 11, the ratio of the ballistic limit to plugging speed needs to be multiplied by a parameter that depends on the ratio of plate thickness to missile radius. This parameter can be determined based on Fig. 10.

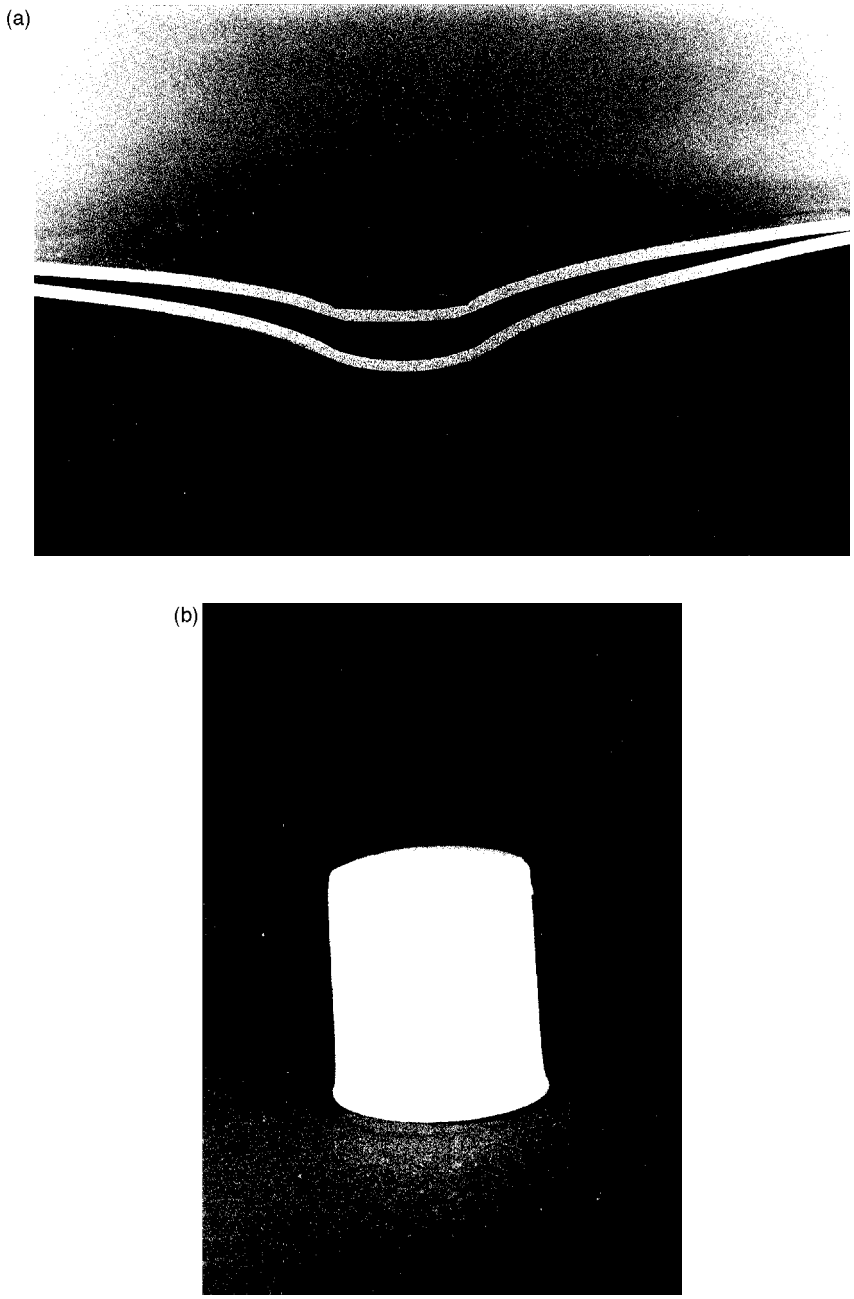

Fig. 7. (a) Final global deflection of 1200 aluminium plates 1.22 mm thick struck by hardened steel and PTFE missiles of equal mass $M = 3.8$ g and radius $H/r_m = 0.195$. The order from top to bottom is a hardened steel missile striking at 94 m/s and a PTFE missile striking at 126 m/s ($\rho_m V_{b1}^2 / Y = 1.6$); (b) the corresponding PTFE missile.

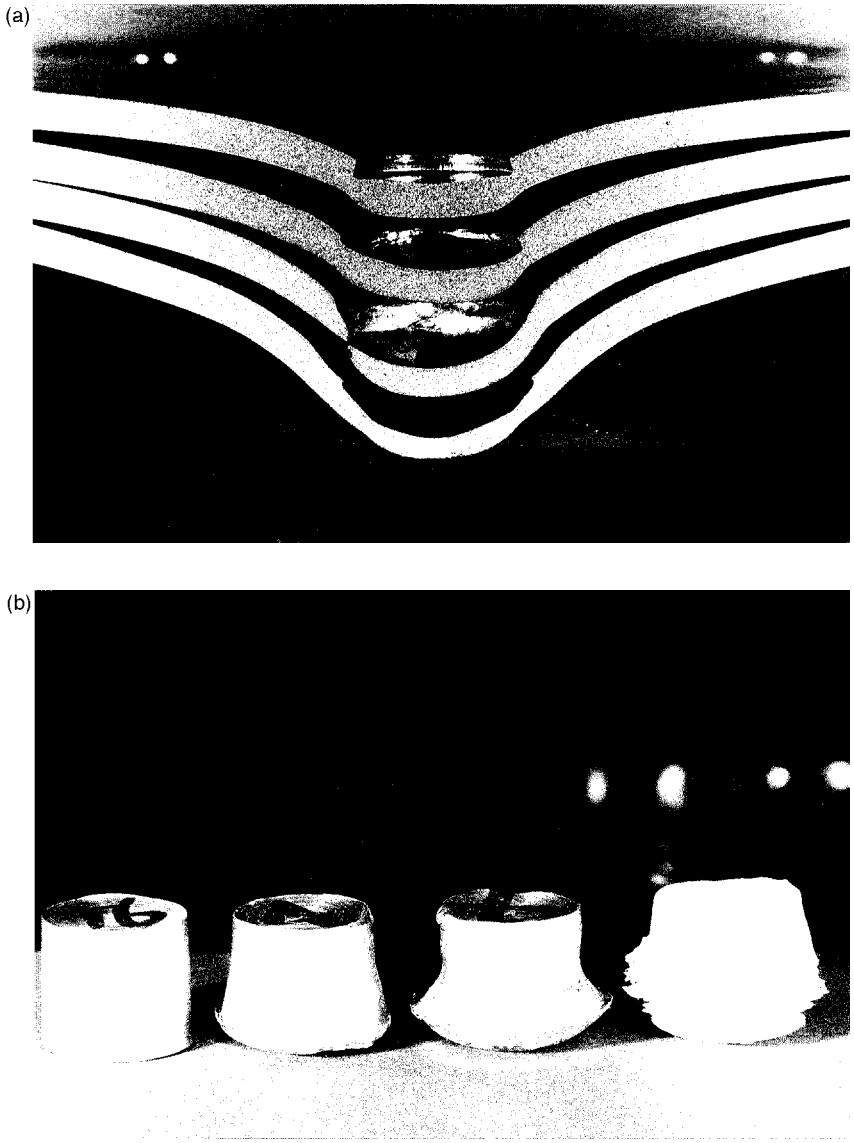

Fig. 8. (a) Final global deflection of 1200 aluminium plates 3.03 mm thick struck by missiles made from materials ranging from PTFE to 6061 T6 aluminium alloy. The missiles have equal mass $M = 3.8$ g and radius $H/r_m = 0.495$. Order from top to bottom is 6061 T6 missile striking at 243 m/s, a 6063 TF aluminium alloy missile striking at 312 m/s, a 1200 aluminium missile striking at 347 m/s and a PTFE missile striking at 400 m/s. With the above order, the value of parameter $\rho_m V_{b1}^2/Y$ changes from 0.45, 0.95, 2.4 to 8.9; (b) from the left to right are the corresponding missiles.

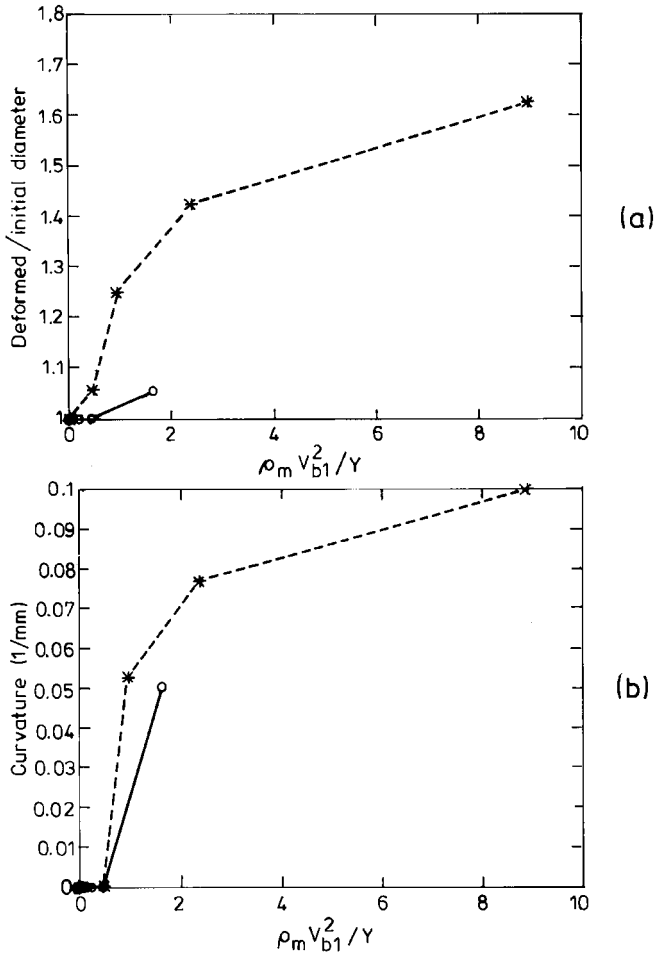

Fig. 9. For the impact end of deformed missiles striking 1200 aluminium plates at the ballistic limit; (a) deformed/initial diameter at impact end and (b) average curvatures at the impact end: —○— plate thickness 1.22 mm ($H/r_m = 0.195$): −−∗−− plate thickness 3.03 mm ($H/r_m = 0.495$). Data points from left to right are for hardened steel, 6061 T6, 6063 TF, 1200 aluminium and PTFE missiles respectively.

failure mechanism is plugging or discing. In the above expression for the local plastic work, σ_0 is static flow stress of the plate. Therefore, for impact of hardened steel missiles, a ratio[4] of the ballistic limit to the minimum speed for plug formation $v_1 \equiv V_{b1}/(2H\sqrt{\pi\sigma_0 e_f r_m/M})$ is proposed to represent the square root of the ratio of total global energy dissipation of a target plate hit at the ballistic limit in comparison with energy required for the same missile to perforate this plate by plugging, $MV_{b1}^2/4\pi\sigma_0 e_f r_m H^2$. The minimum speed for plug formation $V_p \equiv 2H\sqrt{\pi\sigma_0 e_f r_m/M}$ (termed the plugging speed) is the minimum speed for a hard missile to perforate a rigid plastic plate; this impact speed results in perforation only if

[4] This ratio v_1 is equal to the square root of one plus the ratio of the energy absorbed by 'dishing' (plate structural deformation) to the energy absorbed by the local deformation in the narrow hinge band. So the non-dimensional ballistic limit v_1 implicitly incorporates the energy absorbed by 'dishing'.

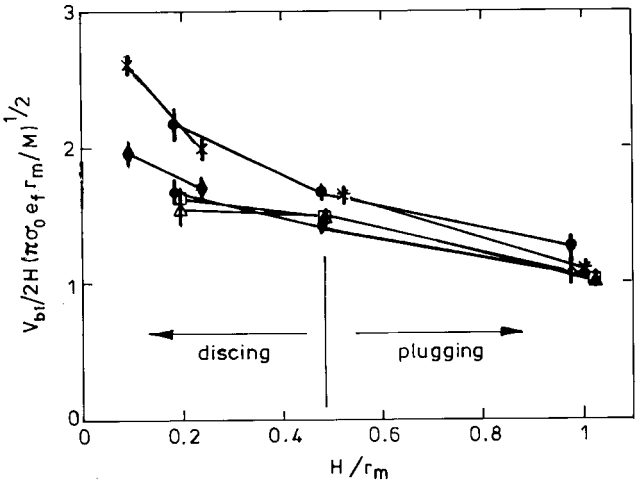

Fig. 10. Variation of the ratio of the ballistic limit to the plugging speed with increasing ratio of plate thickness to missile radius for plates of diameter 95 mm struck by hardened steel missiles: □ 1200 aluminium plates struck by a missile of mass 3.8 g and diameter 12.5 mm: △ 1200 aluminium plates struck by a missile of mass 9.7 g and diameter 12.5 mm: ★ 2014A TB aluminium alloy plates struck by a missile of mass 23.6 g and diameter 12.5 mm: ● mild steel plates struck by a missile of mass 23.6 g and diameter 12.5 mm: × mild steel plates struck by a missile of mass 23.6 g and diameter 25 mm: ○ modification with a dynamic flow stress for mild steel plates struck by a missile of mass 23.6 g and diameter 12.5 mm: ◇ modifications with a dynamic flow stress for mild steel plates struck by a missile of mass 23.6 g and diameter 25 mm.

there is negligible deformation of the plate outside the hinge band. The ratio of the ballistic limit to the plugging speed $v_1 \equiv V_{b1}/(2H\sqrt{\pi\sigma_0 e_f r_m/M})$ is used to explain how the plate yield stress, fracture strain, plate thickness, plate radius, missile mass and missile radius affect the ballistic limit.

The ratio of the ballistic limit to the plugging speed v_1 is plotted as a function of the ratio of plate thickness to missile radius (Fig. 10). Because mild steel is sensitive to strain rates, in Fig. 10 the data for mild steel plates have been adjusted to account for the strain rates; these modified data are calculated with the dynamic flow stress σ_0^d from the eqns in Appendix B. Modified data for aluminium alloy plates are not presented because the difference between the original and modified data is less than 2%.

An important feature of Fig. 10 is that curves for different materials are very close to each other. This means that for a certain value of the ratio of plate thickness to missile radius, the ratio of the ballistic limit to plugging speed is approximately a constant which is independent of missile mass, plate flow stress and plate fracture strain. Thus for a constant value of the ratio of plate thickness to missile radius, $V_{b1} \propto 1/\sqrt{M}$, $\sqrt{e_f}$, $\sqrt{\sigma_0^d}$. Shadbolt et al. (1983) concluded that for mild steel of thickness 1.2 mm, the missile incident kinetic energy at the ballistic limit was approximately a constant for varying missile mass if the missile radius was constant.

Another important feature of Fig. 10 is that the ratio of the ballistic limit to the plugging speed decreases with the ratio of plate thickness to missile radius H/r_m and approaches one as H/r_m approaches one. Recalling the physical meaning of the ratio of the ballistic limit to the plugging speed, the above statement implies that the global energy dissipation of a target plate in comparison to the local plastic work in the hinge band is larger if the plate is thin in comparison with the missile radius. In contrast the global deformation is very small for moderately thick plates ($H/r_m > 0.5$) and rupture is predominantly by plugging.

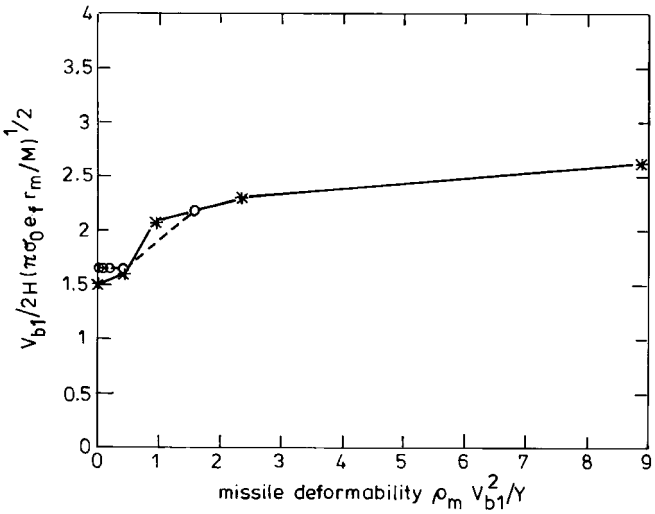

Fig. 11. Non–dimensional ballistic limit of 1200 aluminium plates $v_2 = V_{b2}/(2H\sqrt{\pi\sigma_0 e_f r_m/M})$ as function of the missile deformability $\rho_m V_{b1}^2/Y$. $H = 1.22$ mm – –○– – $H = 3.03$ mm —∗—. Data points from left to right are for hardened steel, 6061 T6, 6063 TF, 1200 aluminium and PTFE missiles respectively.

4.2. Effect of missile deformability

The deformability of a ductile missile striking a ductile metal plate is described by the missile deformability index $\rho_m V_{b1}^2/Y$ which was proposed in Section 3.3. To examine how the deformability of a ductile missile affects the ballistic limit of a target plate, the ratio of the ballistic limit to the plugging speed for a rigid missile $V_{b2}/(2H\sqrt{\pi\sigma_0 e_f r_m/M})$, is taken as a function of missile deformability index (Fig. 11); the symbol V_{b2} denotes the ballistic limit of a plate struck by a deformable missile. The data presented in Fig. 11 are for 1200 aluminium plates with thicknesses 1.22 and 3.03 mm struck by missiles with a deformability index in the range $0 < \rho_m V_{b1}^2/Y < 9$. To further identify the energy dissipation mechanism of a plate struck by a ductile missile at the ballistic limit, the work done to plastically deform a ductile missile during mushrooming is calculated.

Fig. 11 shows that with increasing deformability index, the ratio of the ballistic limit to the plugging speed for a rigid missile has a very similar variation for 1200 aluminium plates of thicknesses 1.22 mm ($H/r_m = 0.195$) and 3.03 mm ($H/r_m = 0.485$). If the deformability index is less than 0.45, the ratio of the ballistic limit to the plugging speed varies little with increasing missile deformability index. Our experiments show that if $0.45 < \rho_m V_{b1}^2/Y$, the ratio of the ballistic limit to the plugging speed increases gradually with increasing missile deformability index. For plates of thickness 1.2 mm ($H/r_m = 0.195$) struck by missiles made from aluminium alloys with different hardnesses, the ballistic limit presented in Fig. 11 equals that of the same plate struck by a hardened steel missile. This is because at impact velocities around 100 m/s, the increase in radius of these missiles is negligibly small (less than 1%) so their ballistic limit speeds are very close to those of a hardened steel missile.

A plate impacted by a ductile missile has a very large ballistic limit in comparison with that for a hardened steel missile because of two factors; i.e. absorption of the missile incident energy by missile deformation and by a large global deformation of the target plate. The latter is due to the enlarged contact area between the missile and plate and our conjecture is that it also is due to the rounded nose shape of a mushroomed missile (Figs 7b and 8b). The plastic work absorbed by a missile E_b^m was estimated using the method presented in Appendix C. Fig. 12 shows the calculations of the ratio of the

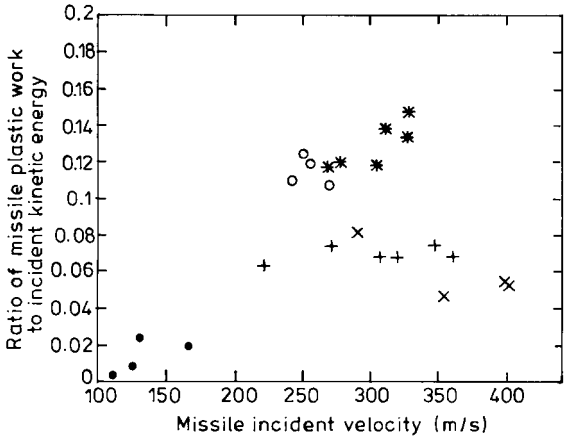

Fig. 12. Ratios of plastic work absorbed by mushrooming of missile to incident kinetic energy at impact speeds near the ballistic limit of 1200 aluminium plates: ○ 6061 T6 missiles striking a 3.03 mm thick plate: ∗ 6063 TF aluminium alloy missiles striking a 3.03 mm thick plate: + 1200 aluminium missiles striking a 3.03 mm thick plate: × PTFE missiles striking a 3.03 mm thick plate: • PTFE missiles striking a 1.22 mm thick plate.

missile plastic work for various deformed missiles as a part of the incident kinetic energy at impact velocities approximately equal to the ballistic limit of 1200 aluminium plates.

To show how the deformability of a ductile missile affects the ballistic limit in comparison with that for a hardened steel missile of the same mass and radius, an increment expression for missile incident kinetic energy δE_b is employed. The increment of missile incident kinetic energy at the ballistic limit is $\delta E_b = E_{b2} - E_{b1}$ where symbols E_{b2} and E_{b1} are respectively the missile incident kinetic energies for ductile and very hard missiles of the same mass and initial radius striking at the ballistic limit. With respect to the large permanent deformation of both missile and target for a ductile plate struck by a soft

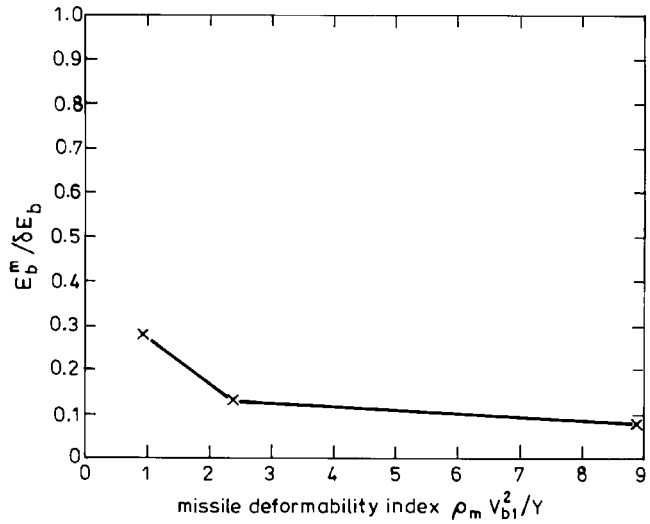

Fig. 13. Variation of non-dimensional energy with the parameter $\rho_m V_{b1}^2/Y$ for 1200 aluminium plates 3.03 mm thick: –X– ratio of missile plastic work E_b^m to increase in incident kinetic energy due to missile deformability δE_b. Datum points from left to right are for 6063 TF, 1200 aluminium and PTFE missiles respectively.

missile, the increment of missile incident kinetic energy is approximately $\delta E_b \approx E_b^m + \delta E_b^p$, here the symbol E_b^m represents the energy absorbed by the plastic deformation of the ductile missile and δE_b^p is the difference between the work done to plastically deform two identical plates struck respectively by ductile and very hard missiles at the ballistic limit. Fig. 13 illustrates the variation of $E_b^m/\delta E_b$ with the missile deformability index $\rho_m V_{b1}^2/Y$ for a 1200 aluminium plate of thickness 3.03 mm[5]. The data for plates 1.22 mm thick is not shown in Fig. 13 because for this plate thickness only the PTFE missile had significant deformation when it struck at velocities close to the ballistic limit.

From Fig. 12 it is known that plastic deformation of the missile absorbs a very small fraction of the missile incident kinetic energy at the ballistic limit. Figure 13 shows that the work done to deform the missile plastically at the ballistic limit is also small in comparison with the increment of missile incident kinetic energy δE_b (about 20%). Because of the increase in the energy consumed by the plate plastic deformation $\delta E_b^p \approx \delta E_b - E_b^m$, the above statement means that the extra permanent deformation of a target plate due to the missile deformability accounts for most of the missile incident kinetic energy δE_b. Combining the above discussion with Fig. 11, we can conclude that a large ratio of the ballistic limit to the plugging speed for a soft missile in comparison with that of a hardened steel missile of same mass and initial radius was mainly due to a very large plate deformation. As shown in Fig. 10, a large ratio of the ballistic limit to the plugging speed corresponds to a large global deformation.

5. Conclusions

1. For a plate that is struck by a flat-ended missile at velocities near the ballistic limit at a normal angle of obliquity, the failure mechanism of a plate changes from discing to plugging as the ratio of the plate thickness to missile radius increases. An analysis by Liu (1996) shows that mild steel and 1200 aluminium plates fail by discing if $H/r_m < 0.5$ and by plugging if $H/r_m > 0.5$. For 2014A TB aluminium alloy, rupture occurs by discing in the range $H/r_m < 0.59$ while plugging occurs in the range $H/r_m > 0.59$.
2. For metal plates struck by hardened steel missiles, a ratio of ballistic limit to plugging speed $v_1 \equiv V_{b1}/(2H\sqrt{M\pi\sigma_0^d e_f r_m/M})$ has been proposed that represents the energy absorbed at the ballistic limit in comparison with local plastic work in a generalised hinge band of width H. Based on our experimental data, it is concluded that this ratio of ballistic limit to plugging speed increases significantly as the plate thickness changes from very thin to almost equal to the missile radius. This occurs because at velocities close to the ballistic limit the global deformation of a target plate increases significantly with decreasing ratio of plate thickness to missile radius (Fig. 3). However, the ratio of the ballistic limit to the plugging speed is very weakly dependent on the missile mass and plate fracture strain. For a constant value of the ratio of plate thickness to missile radius, the ballistic limit $V_{b1} \propto \sqrt{\sigma_0^d e_f/M}$.
3. A missile deformability index $\rho_m V_{b1}^2/Y$ has been proposed that represents the missile mushrooming at the ballistic limit V_{b1}. It is found that if the index $\rho_m V_{b1}^2/Y$ is less than 0.45, the mushrooming of a ductile missile striking at a velocity close to the ballistic limit hardly affects the deformation and failure behaviour of the target plate and consequently the ballistic limit. For $\rho_m V_{b1}^2/Y > 0.45$, the missile is soft and the target plate is more likely to rupture by discing. It has been shown that the plastic work done by mushrooming is very small in comparison with the missile incident energy at the ballistic limit. The increase in the ballistic limit for a very soft missile in comparison with that for a

[5] The datum for the 6061 T6 aluminium alloy missile is not presented because the estimated work done to deform the missile plastically may not be accurate for the small mushrooming that was measured.

hard missile striking the same plate is predominantly due to the increase in the global plastic deformation of the plate. Our conjecture is that the part of the initial missile kinetic energy that is absorbed by the global deformation (dishing) is larger for soft missiles because (a) missile mushrooming increases the plug diameter and (b) the mushroomed nose has a larger curvature at the periphery of the contact region and this reduces the shear strain in the hinge band.

Appendix A: estimate for the average strain rate of a missile

It was assumed that a missile of initial length L was deformed into a frustum of a cone of length L_f. The average strain of the deformed part was estimated by $e_m = (L - L_f)/(L - X)$ where X was the final length of rigid remainder of the missile. The time for a plastic wave advancing from the impact end to an undeformed distance $L - X$ away from the impact end was $T = (L - X)/C_p$ where $C_p (= \sqrt{P/\rho_m})$ is the plastic wave speed in the undeformed material. The average strain rate $\dot{e}_m$ was estimated by $\dot{e}_m = e_m/T$; this gives

$$\dot{e}_m = \frac{(L - L_f)C_p}{(L - X)^2} \tag{4}$$

In this paper, the average strain rate $\dot{e}_m$ is taken as 10^3/s for PTFE missiles because the estimated strain rates are of order 10^3/s.

Appendix B: estimate for the average strain rate of a target plate

Deformed profiles of metal plates struck by a missile at a speed close to the ballistic limit show that the large deformation mainly occurs in a region nearby the generalised hinge band. Consequently we approximate the average strain rate of a target plate with the average strain rate in the generalised hinge band. This gives a upper bound estimate for the average strain rate of the target plate. If the plate centre is assumed to be uniformly decelerated, the average strain rate $\dot{e}_m$ is estimated from the following formula

$$\dot{e}_m = e_f/T_m, \quad T_m = 2\delta_f/V_0 \tag{5}$$

where e_f is the fracture strain of a target plate, δ_f is the final central deflection of a plate struck by a hardened steel missile at a velocity V_0 just below the ballistic limit (see the inset figure of Fig. 3). In the generalised hinge band, the material is assumed to fail when the effective strain reaches the fracture strain e_f (Liu, 1996; Shen and Jones, 1992, 1993). In perforation tests performed by Langseth and Larsen (1990, 1994) it was found that through thickness rupture in target plates occurred approximately at the maximum indentation force. At the maximum indentation force, there was no obvious unstable deformation stage in the indentation force–deflection curves (see Liu, 1996). A similar method employing a homogeneous strain-rate effect was used by Shen and Jones (1992, 1993) and this gave a credible estimate of the effect of strain rates on dynamic flow stress in their calculation.

Appendix C: plastic work done by a missile

The plastic work absorbed by a cylindrical missile is estimated using Johnson's model (Johnson, 1972)

which assumes that the cylinder deforms to a frustum of a cone and that the missile material is rigid perfectly-plastic. The expression for plastic work absorbed by a missile is

$$E_{\mathrm{b}}^{m} = \int_V Y\varepsilon \,\mathrm{d}V$$

$$= \int_V Y \ln \frac{A}{A_0} \,\mathrm{d}V$$

$$= Y \frac{2\pi(L_{\mathrm{f}} - X)r_m^3}{9(r_{\mathrm{f}} - r_m)} \left[3\left(\frac{r_{\mathrm{f}}}{r_{\mathrm{m}}}\right)^3 \ln\left(\frac{r_{\mathrm{f}}}{r_{\mathrm{m}}}\right) - \left(\frac{r_{\mathrm{f}}}{r_{\mathrm{m}}}\right)^3 + 1 \right] \tag{6}$$

where Y is the missile yield strength, ε is missile true strain, X is the final height of undeformed part, L_{f} is the final height of the whole missile, r_{m} is initial missile radius and r_{f} is final radius of the deformed (impact) end. The dynamic yield stress estimated in Appendix A is used in calculating the plastic work absorbed by PTFE missiles because PTFE is very sensitive to strain rates. The final height of the mushroom $(L_{\mathrm{f}} - X)$ and radius of the deformed (impact) end r_{f} were estimated by averaging mushroom height and diameter of the missiles obtained from incident velocities on either side of the ballistic limit.

References

Backman, M.E., Goldsmith, W., 1978. The mechanics of penetration of projectiles into targets. Int. J. Engng. Sci. 16, 1–99.

Corbett, G.C., Reid, S.R., Johnson, W., 1996. Impact loading of plates and shells by free-flying projectiles: a review. Int. J. Impact Engng. 18, 141–230.

Corran, R.S.J., Shadbolt, P.J., Ruiz, C., 1983. Impact loading of plates, an experimental investigation. J. Impact Engng. 1, 3–22.

Dienes, J.K., Miles, J.W., 1977. A membrane model for the response of thin plates to ballistic impact. J. Mech. Phys. Solids 25, 237–256.

Johnson, W., 1972. Impact strength of materials. Edward Arnold, London.

Jones, N., Kim, S.B., Li, Q.M., 1995. Response and failure analysis of ductile circular plates struck by a mass. University of Liverpool, Impact Research Centre Report No. IRC/110/93.

Langseth, M., Larsen, P.K., 1990. 'Dropped objects' plugging capacity of steel plates: an experimental investigation. J. Impact Engng. 9, 289–316.

Langseth, M., Larsen, P.K., 1994. 'Dropped objects' plugging capacity of aluminium alloy plates. J. Impact Engng. 14, 225–241.

Lethaby, J.W., Skidmore, J.C., 1974. The deformation and plugging of thin plates by projectile impact. In: Harding, J. (Ed.), Conference on the Mechanical Properties of High Strains, Conference Series, No. 21. Institute of Physics, London, pp. 429–441.

Lindholm, U.S., 1964. Some experiments with the split Hopkinson pressure bar. J. Mech. Phys. Solids 12, 317–335.

Liu, D., Stronge, W.J., 1995. Perforation of rigid plastic plate by blunt missile. Int. J. Impact Engng. 15, 739–758.

Liu, D., 1996. Penetration and Perforation of Metal Plates Struck by Deformable Missiles. PhD Dissertation, Cambridge University, Engineering Department.

Palomby, C., Stronge, W.J., 1988. Blunt missile perforation of thin plates and shells by discing. Int. J. Impact Engng. 7, 85–100.

Recht, R.F., 1978. Taylor ballistic impact modelling applied to deformation and mass loss determinations. Int. J. Eng. Sci. 16, 809–827.

Shadbolt, P.J., Corran, R.S.J., Ruiz, C., 1983. A comparison of plate perforation models in the subordnance impact velocity range. Int. J. Impact Engng. 1, 23–49.

Shen, W.Q., Jones, N., 1992. A failure criterion for beams under impulsive loading. Int. J. Impact Engng. 12, 101–122.

Shen, W.Q., Jones, N., 1993. Dynamic response and failure of fully clamped circular plates under impulsive loading. Int. J. Impact Engng. 13, 259–278.

Stronge, W.J., 1995. Impact and perforation of cylindrical shells by blunt missiles. In: Reid, S.R. (Ed.), Metal Forming and Impact Mechanics. Pergamon Press, Oxford, pp. 289–302.

Swallow, G.M., Field, J.E., Horn, L.A., 1986. Measurements of transient high temperatures during the deformation of polymers. J. Mat. Sci. 21, 4089–4096.

Taylor, G.I., 1948. The use of flat-ended projectiles for determining dynamical yield stress, I. theoretical consideration. Proc. R. Soc. London A 194, 289–299.

Walley, S.M., Field, J.E., Pope, P.H., Safford, N.A., 1989. A study of the rapid deformation behaviour of a range of polymers. Phil. Trans. R. Soc. London A 328, 1–33.

Wen, H.M., Reddy, T.Y., Reid, S.R., 1995. Deformation and failure of clamped beams under low speed impact loading. Int. J. Impact Engng. 17, 435–454.

Whiffin, A.C., 1948. The use of flat-ended projectiles for determining dynamical yield stress, II. Test on various metallic materials. Proc. R. Soc. London A 194, 300–322.

Woodward, R.L., 1979. Penetration behaviour of a high strength aluminium alloy. Metals Tech 6, 106–110.

Woodward, R.L., DeMorton, M.E., 1976. Penetration of targets by a flat-ended projectile. Int. J. Mech. Sci. 18, 119–127.